Journal of Alloys and Compounds 506 (2010) 645–652

Contents lists available at ScienceDirect

Journal of Alloys and Compounds

journal homepage: www.elsevier.com/locate/jallcom

Microstructure, mechanical properties and wear behavior of metallic, nonmetallic and deep cryogenically chilled ASTM A216 WCB steel

Joel Hemanth*

Akshaya Institute of Technology (A.I.T.), Lingapura, Obalapura Post, Tumkur-Koratagere Road, Tumkur 572106, Karnataka, India

ARTICLE INFO

Article history:
Received 29 January 2010
Received in revised form 1 July 2010
Accepted 7 July 2010
Available online 15 July 2010

Keywords:
Mechanical properties
Microstructure
Heat capacity
Metallography

ABSTRACT

This paper deals with the production of Deep Cryogenically Chilled (DCC) ASTM A216 WCB steel (plane carbon group) having 0.5% chromium, subject to different chilling rates to study the effect of chilling on microstructure and mechanical properties. In this investigation, metallic, nonmetallic and subzero chills (one each) were used. The specimens taken from casting were tested for their strength, hardness and wear behavior. Results of the investigation reveal that chilling rate and addition of chromium (0.5%) has improved both mechanical properties (strength and hardness) and wear resistance of the steel developed. Out of all the chills, subzero chill is found to be good in improving mechanical properties because of its high volumetric heat capacity (VHC). It is concluded from the above investigation that type of chill and chilling rate has an effect on mechanical properties.

1. Introduction

Steel is a material known for its strength and ductility. The combination of strength and ductility adds to give steel greater values of toughness and resistance to shock. It is well known that, properties of steel can be controlled by controlling its composition or by heat treatment.

In a study on effect of high rate heat transfer during solidification of alloyed cast iron using water-cooled and subzero chills on mechanical behavior [1] it is concluded that number of eutectic cells was significantly larger in the case of chilled cast iron than that obtained in the case of cast iron cast without a chill. Eutectic cell count was shown to be a major factor that affects ultimate tensile strength and fracture toughness. In another study on microstructure of cryogenically treated M2 tool steel [2] it is reported that, cryogenic treatment facilitate the formation of carbon clustering and subsequent heat treatment improves the wear resistance of steel.

Collins and Dormer [3] has studied the effect of Deep Cryogenically Treated (DCT) D2 cold work tool steel and found that, DCT steels give lowest wear rate compared to conventionally heat treated steels. Barron [4] conducted some preliminary tests to determine the effect of cryogenic treatment on lathe tools, end mills and found that there is an increase in tool life from 25% to 35% when soaked in liquid nitrogen for 12 h. Meng and Tagashira [5] studied the wear resistance of Fe–12Cr–Mo–V–1.4C tool steel both with and without cryogenic treatment. Their study reveals that, conventionally heat treated and cryogenically treated specimens showed smaller wear volume at all sliding distances. Bensely et al. [6] made comparative study on wear resistance improvement of DCT and Shallow Cryogenic Treatment (SCT) using pin-on-disc wear tester. They found that, although the hardness value between the SCT and DCT samples are the same, wear resistance of DCT samples are high compared with SCT samples, which is due to precipitation and finer distribution of carbides. In a study on wear and corrosion wear of medium carbon steel it was found that, the samples showed smaller weight loss and lower friction coefficient in the presence of corrosive environment [7]. In another investigation it was shown that, wear resistance improved dramatically through thermo-mechanical treatment due to elimination of porosity [8]. It was also demonstrated in other research that, wear rate is largest in the as cast form having highest weight loss [9]. Hence in the present investigation, cryo-chilling route during solidification, followed by aging is adopted to eliminate microporosity and to improve mechanical properties [10,11].

1.1. Relevance of the present research

The objective of the present research is to examine the effect of microalloying (0.5% Cr) on the microstructure and mechanical properties of chilled ASTM A216 WCB steel which belong to plain carbon group. These steels are widely used in the production of valves, flanges, motor casing, rollers for crushing ores and fittings for high temperature service. So for no work has been done on

* Fax: +91 816 2245777.
E-mail address: joelhemanth@hotmail.com.

0925-8388/$ – see front matter © 2010 Elsevier B.V. All rights reserved.
doi:10.1016/j.jallcom.2010.07.036

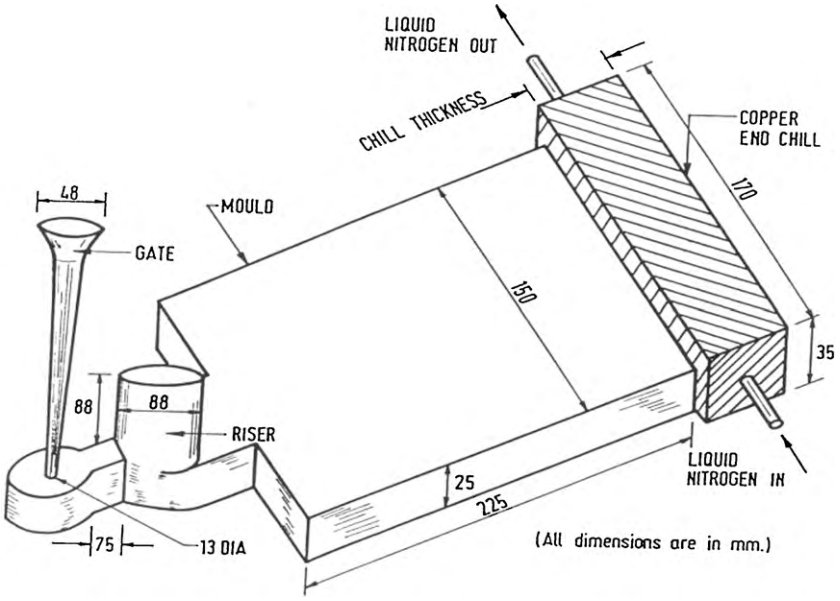

Fig. 1. Experimental setup for production of cryo-chilled steels.

cryogenically treated steel during solidification on A216 WCB steel. Hence the present work is under taken to fill the void.

2. Experimental procedure

2.1. Molding, melting and casting

In the present research, metallic, nonmetallic and subzero copper end chills were used to get test castings. These end chills were fabricated to required size and set in CO_2 sand molds (AFS standard size 225 mm × 150 mm × 25 mm) with arrangements made to circulate liquid nitrogen (for cryo-effect) at −90 °C (Fig. 1). Zircon sand coating was applied to mold to get good surface finish as well to avoid fusing of sand.

Chills used:

1. Subzero copper chill
2. Metallic chill (copper)
3. Nonmetallic chill (graphite)

Steel alloy having the composition of ASTM A216, WCB grade with 0.5% Cr addition was melted in an induction furnace. The melt was superheated to 1640 °C and is taken into a preheated ladle containing calcium silicide (which acts as deoxidizing agent) during pouring. Finally, the treated molten metal was poured into the mold (at 1625 °C) containing different end chills. After solidification all the test castings were heat treated (aging) for 5 h and finally these castings were cleaned and cut to prepare specimens. The chemical composition of steel used in the present investigation is as shown in Table 1.

2.2. Testing

2.2.1. Tensile and hardness tests

Tension tests were conducted at ambient temperature on computerized universal testing machine of 60 ton capacity in the load range of 0–600 kN. The specimens for mechanical tests were selected at three different locations along the length of the casting (at 15, 110 and 210 mm from chill end) and were prepared according to AFS standards. Rockwell hardness (HRB) for the sample was measured using ZWICK-Roll ZHR hardness tester with a load of 100 kg-f using ball indenter of size 1/16 inch in diameter. The values reported in both of these tests are the average of three repetitions on the same sample at the same location.

2.2.2. Sliding wear test

Wear test for the samples are conducted using pin-on-disc computerized (DUCOM make) wear testing machine. The specimen is a pin of size 6 mm in diameter and 25 mm long where as the disc is of alloy steel having hardness of HRC 62. Before the test the surface of the pin was cleaned with acetone and volume loss method (LVDT attached to the specimen used to measure change in length) was adopted to ascertain wear loss. Test was carried out by applying normal load on pin from 10 to 30 N in steps of 10 N at different disc speeds.

2.2.3. Metallographic examination

The specimens for microstructural studies were polished according to metallurgical standards and fine polishing was done using alumina powder and diamond paste. The specimens were etched with 3% Nital to evolve grain boundaries. Microstructural studies were done using Olympus optical metallurgical microscope. SEM is used to study the worn surface as well as the wear morphology of the worn surface.

3. Results and discussions

3.1. Mechanical properties (strength and hardness)

Results of mechanical tests (strength and hardness) are shown in Figs. 2 and 3. It is seen from these figures that strength and hardness both decrease along the length of the casting from chill end to the riser end. It is observed from Figs. 2 and 3 that strength and hardness of WCB steel cast with subzero chill is found to be superior compared to steel cast using other type of chills. Improvement in strength and hardness in the case of subzero chilling is because of high volumetric heat capacity (VHC) of the chill. This has resulted in carbide formation in fine pearlitic matrix (see Fig. 5a) during solidification. It is finally observed that addition of chromium (0.5%) to base WCB steel and cryo-chilling increases strength by 20 N/mm^2 and hardness by 4 HRB near the chill end as compared with un-chilled steel.

Fig. 4a and b shows SEM fractographs of subzero chilled and un-chilled steel specimens failed in tension testing. It is seen from the fractographs that subzero chilled steel has fine grain structure with large dimples as compared with un-chilled steel which has shallow dimples. It is also observed that the mode of fracture has changed from moderately ductile (un-chilled) to cleavage in the case of subzero chilled WCB steel.

Table 1
Chemical composition of ASTM A216 WCB steel (wt.%).

Element	C	Si	Mn	P	S	Cr	Mo	Ni	Fe
Composition	0.235	0.351	0.994	0.034	0.012	0.234	<0.001	0.014	Balance

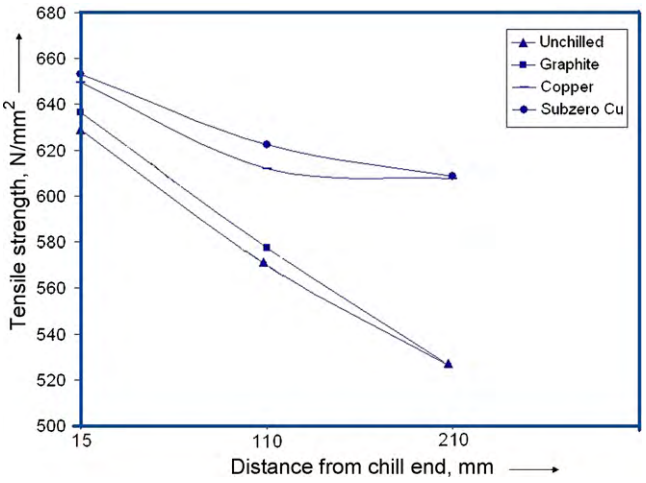

Fig. 2. Ultimate tensile strength of different steels along the length of the casting.

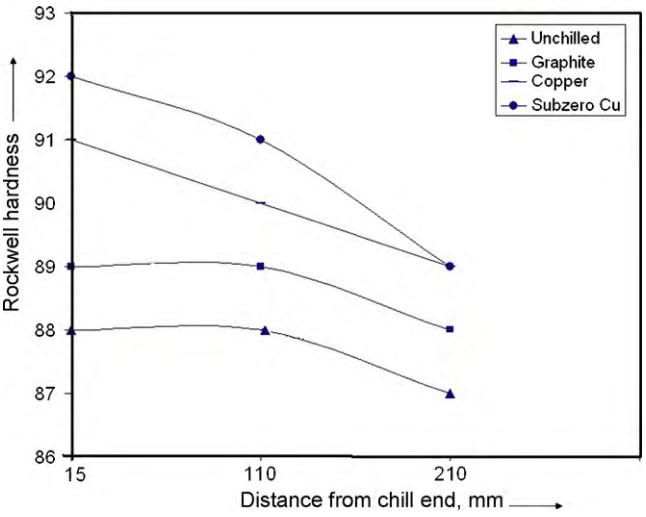

Fig. 3. Hardness (HRB) of different steels along the length of the casting.

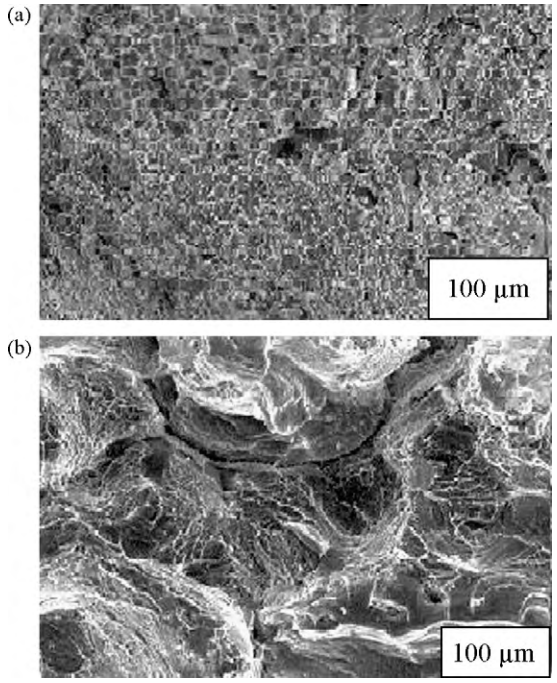

Fig. 4. Fractured surface of specimens failed in tension.

3.2. Microstructural observation

3.2.1. Solidification pattern

Fig. 5a–d shows microstructure of WCB steel cast using different chills, Fig. 5e and f shows eutectic cell count (at low magnification, 50×) and Fig. 5g and h shows dendrite arm spacing (DAS) of un-chilled and subzero chilled steel. The differences in associated graphite, its randomness, length and matrix structure (as shown in Fig. 5a–d) for the various steels cast were analyzed and correlated to the temperature of eutectic formation. Faster cooling produces fine, highly oriented dendrites, while slow cooling produces large, coarse dendrites. Solidification over a temperature range is the primary requirement for dendrite growth. Primary austenite dendrites readily grow from the liquidus down to the eutectic temperature. Growth of dendrites may also continue concurrently with the eutectic as the temperature decreases through eutectic range to the solidus. Thus, under-cooling in case of liquid–nitrogen-cooled (subzero chilled) steel may lead to longer dendrites and higher interaction. Hence, the eutectic cells solidify around these austenite dendrites and in this manner the entire microstructure is affected by the number and size of the dendrites.

Therefore the general picture of solidification of un-chilled steel and chilled steel (metallic, nonmetallic and subzero chilled) with various eutectic cells, dendrite arm spacing, graphite shapes and matrix structures (as shown in Fig. 5a–h) can be summarized as follows: the solidification of WCB steel resulting from sand casting without a chill starts from a small number of nuclei as compared with chilled steels, a phenomenon indicated by eutectic cell count (see Fig. 5e and f). Since the growth condition in the liquid are favorable, these nuclei start growing as soon as temperature below the equilibrium temperature in case of sand cast steel (un-chilled) and with maximum under-cooling in the cases of chilled steel, whether metallic or subzero chilled.

3.2.2. Pearlitic content

From the microstructural observations, it can be seen that there exists a straight forward relationship between pearlite content and eutectic cell for the various specimens cast using different type of chills. It is noteworthy that steel cast using subzero chill and metallic chill (cu) contain cementite in fine pearlite matrix whereas un-chilled steel and steel cast using nonmetallic chill (graphite) contain ferrite in coarse pearlite matrix (Fig. 5a–d).

3.2.3. Dendrite formation

Results of the investigation indicate that the minimum eutectic temperature can be used as a measure of under-cooling that reflects DAS (Fig. 5g and h), the number of cells (Fig. 5e and f) precipitated and the chilling tendency of the steel. Higher dendritic interaction areas in the case of chilled steels reflect the interweaving of dendrite through eutectic cells that effectively tie the eutectic cells together. Since dendrites are formed from primary austenite, they have a higher tensile strength than eutectic carbon. Here, due to chilling, dendrites directly form from austenite and do not contain flake carbon. Instead they contain carbides (cementite) in the pearlite matrix as shown in Fig. 5a–d.

3.2.4. Effect of microalloying (0.5% Cr) on microstructure

Fig. 5a–c shows the microstructure of subzero, metallic and nonmetallic chilled ASTM A216 WCB steels containing 0.5% Cr. From these figures it is observed that there is excess carbide formation (nearly 20%) in pearlitic matrix for subzero chilled steel as compared with metallic and nonmetallic chilled steels. Such carbide formation in pearlitic matrix contributes a lot for enhancement in mechanical properties and wear resistance.

Research findings by Meng and Tagashira [5] on steel containing 12% Cr (without chilling) showed nearly 18% carbide formation

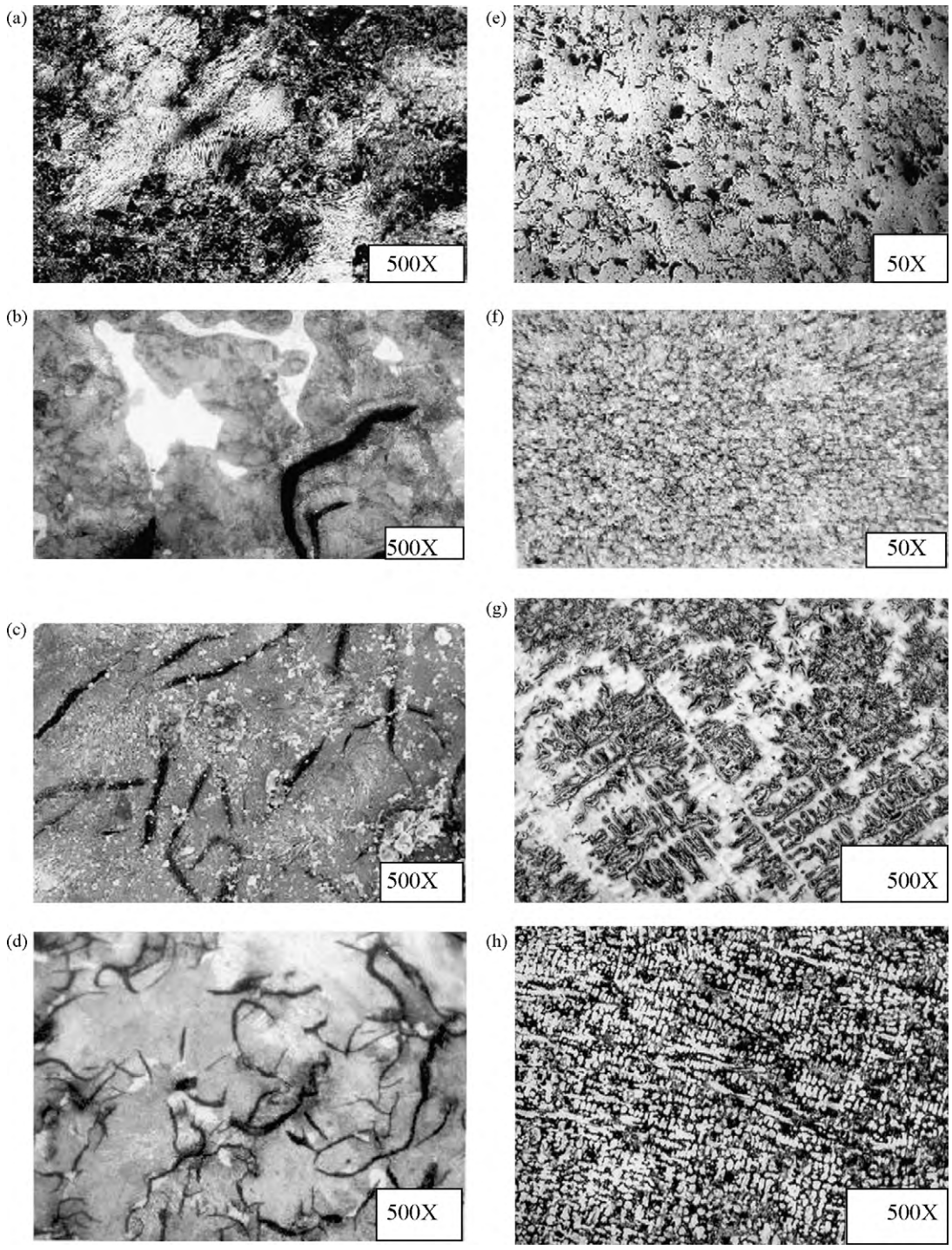

Fig. 5. Microstructure (a–d), eutectic cell (e and f) and dendrite arm spacing (g and h) of different steels.

in peralitic matrix. This shows that microalloying (with 0.5% Cr) the cryo-treated steel has almost the same effect as that of high Cr steels.

3.3. Wear

3.3.1. Friction and wear

Fig. 6 shows the variation in volume loss of the WCB steel as a function of sliding distance tested at a load of 30 N. At the lowest load (10 N, fig. not shown) in mild wear regime with a high coefficient of friction is always found for all the chilled steels tested. At higher loads (30 N), the chilled steels exhibited severe wear with a better wear resistance than the un-chilled steel. Un-chilled and the nonmetallic chilled steels, tested at all loads underwent large volume loss during the early stages of the test. After sliding for some distance, the volume loss increased approximately linear with sliding distance. The sliding distance for transition from severe to mild wear could be identified by two factors: firstly, by abrupt and steep reduction in the frictional force, and secondly, by change in the magnitude of displacement of pin specimen [12]. Based on these measurements, the wear curves are characterized by two distinct lines of different slopes, which correspond to severe and mild wear conditions. Steel, cast under subzero condition showed steady state mild wear from the beginning of the test. At no point during the

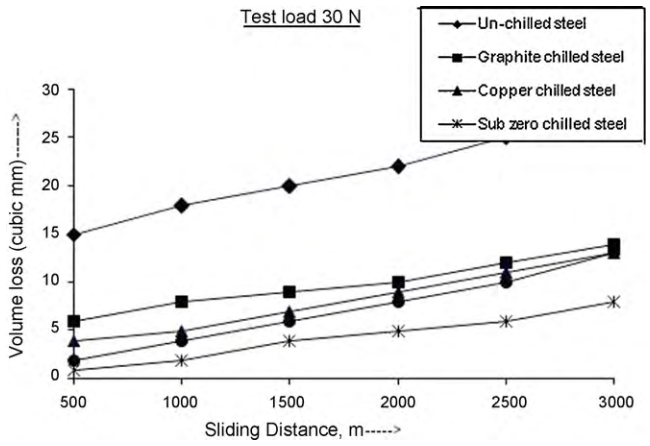

Fig. 6. Plot of volume loss vs. sliding distance for various chilled steels tested under a load of 30 N.

tests, severe wear was noticed. It is also observed that, the sliding distance and volume loss in the severe wear regime decreases with an increase the chilling rate. Therefore, in the case of steels cast under subzero condition, severe wear did not occur at all. The wear rate in the wear regime is calculated by dividing the volume loss by the sliding distance. In the severe wear regime, wear rates of steels decrease with increasing the chilling rate. The transition to lower wear rates (mild wear regime) is accelerated with increasing in heat capacity of the chill. It is obvious that chilling effectively prevents the time/distance required for transition from severe to mild wear.

The mean steady state values of the coefficient of friction (μ) as a function of sliding speed tested at a load of 30 N is reported in Fig. 7 for both the un-chilled and the chilled steels. At the lowest applied load of 10 N (fig. not shown) and at the lowest sliding speed of 0.3 m/s a very high coefficient of friction about 1.0 was measured for the un-chilled steel in the mild wear regime and for the chilled steels it is reduced to around 0.76. At intermediate sliding speed (1.2 m/s) the coefficient of friction decreases in the mild wear regime and finally at higher sliding speeds (1.8 m/s) all the steels displayed the same frictional behavior with coefficient of friction value around 0.55. With an applied load of 20 N (fig. not shown) and at the lowest sliding speed a high coefficient of friction of 0.92 was measured for the un-chilled steel in the mild wear regime, whereas for the chilled steels it is decreased to 0.7–0.87. At the highest applied load of 30 N and at the lowest sliding speed a high

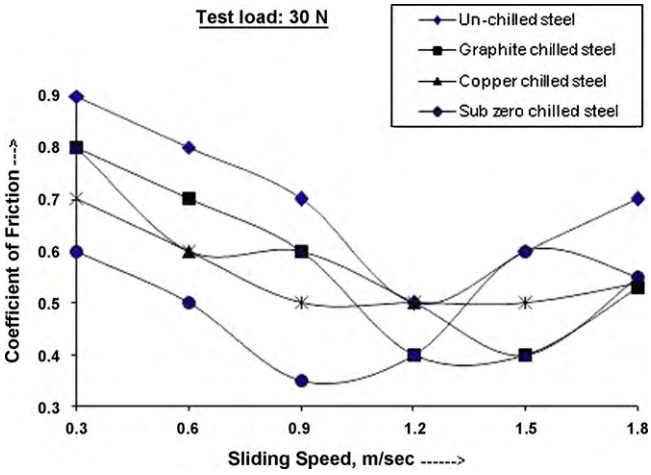

Fig. 7. Plot of coefficient of friction vs. sliding distance for various chilled steels tested under a load of 30 N.

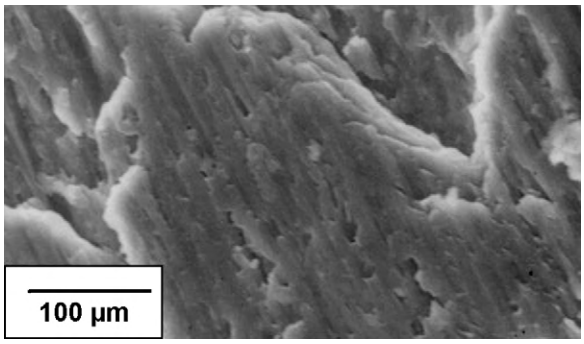

Fig. 8. SEM photograph showing the cross-section parallel to the sliding direction for sun zero chilled steel in the severe wear regime.

coefficient of friction of 0.9 was measured for the un-chilled steel which displayed a mild wear regime, whereas the chilled steels at the same sliding speed was decreased down to 0.6–0.8 as shown in Fig. 7. At intermediate sliding speed the trend is that, a high coefficient of friction was measured in the mild wear regime and decrease to lower values of 0.35–0.5. At the highest sliding speed all the chilled steels displayed the same frictional behavior with a lower value of coefficient of friction around 0.55 independently from the applied load the wear regime.

3.3.2. *Effect of chilling on severe wear*

Subzero chilling changes the microstructure of an un-chilled steel (ferrite in coarse pearlitic matrix to cementite in fine pearlitic matrix) and thus affects wear behavior. The observation made using optical microscope (Fig. 8) clearly reveals cementite contained in fine pearlite matrix is accompanied by the deformation and hence the microcracks. The depths of the deformation zone where the cementite is deformed, was measured in order to obtain the depth of the plough region. These depths were found to be 49 μm for un-chilled steel and 24 μm for cryogenically chilled steel. It is also observed that the depth of the deformation zone decreases with increasing the VHC of the chill. Further, the cracks propagate in the subsurface as a result of adhesion and deformation. In the beginning of the wear test, the plastic flow of the ferrite for steel cast using graphite chill, is appreciable and thus causes severe wear. But in the case of chilled steels, the formation of a hard surface consisting of carbides in pearlitic matrix helps in preventing adhesion. As a result, transition from severe to mild wear occurs and hence the wear rate was reduced as a result of removal of wear debris at lower wear rate. For steels cast using Cu and subzero chills, the deformation is prevented because of the beneficial effects of the grain size. Therefore it is considered that severe wear caused by the adhesion disappears with increasing the chilling rate.

3.3.3. *Effect chilling on mild wear*

Fig. 9a–d shows SEM photograph of the worn surfaces of the un-chilled and chilled steels (cast using different chills) in the mild wear regime. It is observed that for the steel cast using graphite chill, worn surface is completely smooth and flat and contained wear tracks in the direction of sliding. In addition, the signature of plastic flow was not at all observed in the subsurface. In contrast, the worn surface of WCB steel cast using cu chill is found to be rough. Microscopic examination of the subsurface shows fragmentation and uniform dispersion of the entire worn surface and, as a result, plastic flow was very limited. Further, in the case of subzero steel the surface was found to be very rough with a characteristic brittle fracture and the subsurface region consisted of fragments of crushed carbide (indicated by an arrow in Fig. 9d). This shows that mild wear is dominated in steels cast using copper and subzero chills. A very thin tribo-induced layer was formed on

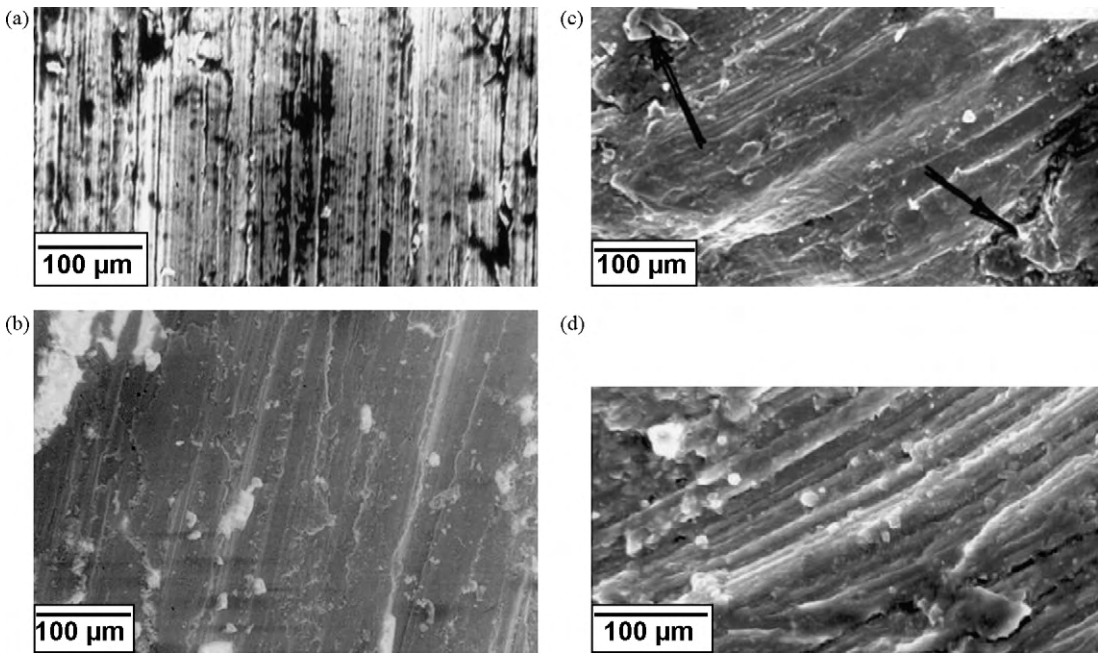

Fig. 9. SEM photomicrograph of worn surface of various steels in the mild wear regime. (a) Un-chilled steel. (b) Graphite chilled steel. (c) Copper chilled steel. (d) Subzero chilled steel.

the entire surface and, in addition some carbide is projected onto the surface. The lengths of the crushed carbides were measured for more than 10 fragments on the several cross-sectional micrographs. The mean length was found to be 8 μm (ranging from 4.5 to 12 μm) for subzero chilled steels. From these detailed observations, it becomes obvious that the carbides present were crushed into small fragments and a thin layer was formed on the smooth surface containing wear tracks confirming abrasive wear in the mild wear regime.

3.3.4. Modes of wear mechanism

Wear mechanism of the present investigation is suggested by two modes. Mode-1 refers to adhesive wear (severe wear) and is predominant in the un-chilled steel and also in steel cast using graphite chill at higher loads. This type of wear disappears as the rate of chilling increases. On the other hand, Mode-2, which is essentially abrasive wear (mild wear) as result of embedded hard carbide particles in steels exposed on the worn surface and the loose fragments between two surfaces, dominates in steels cast using chills of high VHC (copper and subzero chilled steels).

SEM examination reveals that the worn surface of the chilled steel consist of both hardened and deformation layers. The structure of the hardened layer consists mainly of the fragmented carbide phase. The depth of this layer depends on the applied load and is in the vicinity of 10–40 μm. However, the depth of the hardened layer in the steel is markedly reduced by increasing the chilling rate. Moreover, the hardness value of the hardened layer in the chilled steel was considerably higher than that of the un-chilled steel. Fig. 10a and b shows the wear mechanism of chilled steel under mild wear conditions. Because of limited plastic deformation in the mild wear regime of subzero chilled steel the microstructural studies reveal that, the fragmentation of the carbide appears as brittle fracture and in the case of un-chilled steel the plastic flow is due to deformation of ferrite.

3.3.5. Relationship between load, microstructure and wear

In the two-body abrasion, the major portion of the load applied during testing is transferred to the specimen and the wear of the material took place under high stress condition [13]. This is supported by the experimental results, as evident by the increase in transition load from severe to mild wear with the chilling rate [14]. These explanations are in line with earlier reports of Moustafa [15] that have shown an increase in the load for transition from mild to severe wear.

The hard carbide particles in chilled steel act as protuberances in the peralitic matrix and bear the major portion of load and as a consequence, protect steel from wear. This leads to the reduction of wear rate of chilled steel due to reinforcement of carbide particles in the pearlitic matrix of chilled steel. The wear rate is significantly dependent on the applied load, microstructure and hardness of the material. The cutting efficiency of the disc particles increases with an increase in the applied load. As a result, more material was removed at higher loads and hence the wear rate increases with an applied load. The depth and width of cutting grooves also

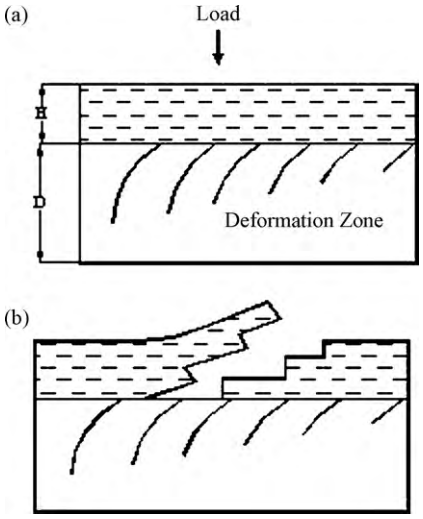

Fig. 10. Schematic diagram showing (a) wear mechanism of chilled steel indicating alignment and redistribution of carbide phase in the deformation zone (*D*) leading to the formation of a hardened surface layer (*H*) and (b) fragmentation of carbide under mild wear condition for subzero chilled steel.

depends on the hardness of the material [16]. The hardness of the un-chilled steel is lower than that of the chilled steels and hence, the wear rate of chilled steels becomes lower than that of the un-chilled steel. Since the chances of fracturing of carbide particles in the pearlitic matrix are less in the case of chilled steels, leads to a higher wear resistance of the cryogenically chilled steels even in high load regime. As a result, the removal of a material vis-à-vis the wear rate of the material is governed by deformation parameters, microstructure and hardness. Thus by increasing the strength and hardness between pearlitic matrix and the carbide particles (effect of chilling), the cutting efficiency of the hard disc particles is reduced.

3.3.6. Relationship between hardness and wear

It is well known that the wear rate of the material decreases with hardness irrespective of the applied load. SEM studies of the chilled steels tested at different loads reveal that, at lower load (10 N), the variation of wear rate with hardness is marginal, but at higher load (30 N) considerable wear with hardness was noted. At lower load, mainly cutting type wear takes place and the subsurface deformation is negligible [17]. The carbide particles remain intact within the pearlitic matrix and protect the specimen surface more effectively. Thus, at lower load, the surface deformation behavior is negligible. At higher load, both cutting and ploughing types of mechanisms are operating and the subsurface deformation becomes considerably high. Because of subsurface deformation, transverse and longitudinal cracks are generated on the wear surface [18]. Subsequently, because of cold working, the subsurface is also work hardened [19]. The subsurface deformation is governed by the mechanical properties such as hardness, ductility and strength, which are again influenced by the microstructure and distribution of hard carbide particles. These may cause considerable reduction in the wear rate with an increase in hardness and strength when tests are conducted at higher applied load. The subsurface deformation of the un-chilled steel may vary because of different matrix microstructure and mechanical properties. In addition to initial hardness of the chilled steel, after a few cycles of motion of the sample against the abrasive media, the hardness of the wear surface of different samples increases. Apart from this, since the carbide particles are very fine (Fig. 5) and they may have the tendency to break into small particles and spread over the wear surface thus protecting the pearlitic matrix from severe wear. Fig. 11 shows the photomicrograph of fragmented carbide particles in the subsurface region for subzero chilled steel in severe wear regime. This includes higher hardness of the surface of the chilled samples than their bulk hardness during testing. This in turn results in a significantly lower wear rate in the chilled steels as compared as compared to the un-chilled steel and chilled steels at higher applied loads. The cracking and removal of flaky materials and work hardening of the subsurface take place simultaneously over the specimen surface. The overall wear rate of the material would depend on the cutting action and work hardening rate of the chilled steels may be higher and it increases with an increase in hardness. Apart from this, the possibility of fracture and fragmentation of carbide particles may be low in chilled steels because of the strong and hard carbides in the pearlitic matrix due to the effect of cryo-chilling. In fact the wear characteristics of the chilled steels are governed by the interaction of their chilling effect and hardness.

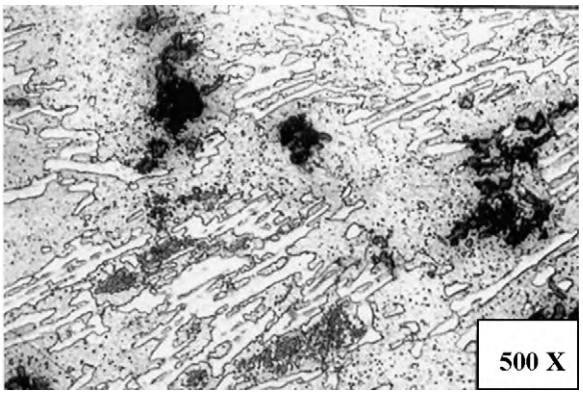

Fig. 11. SEM photomicrograph of subsurface deformation of cryo-chilled steel showing deformed region depicting the fragmentation of carbide particles in the severe wear regime.

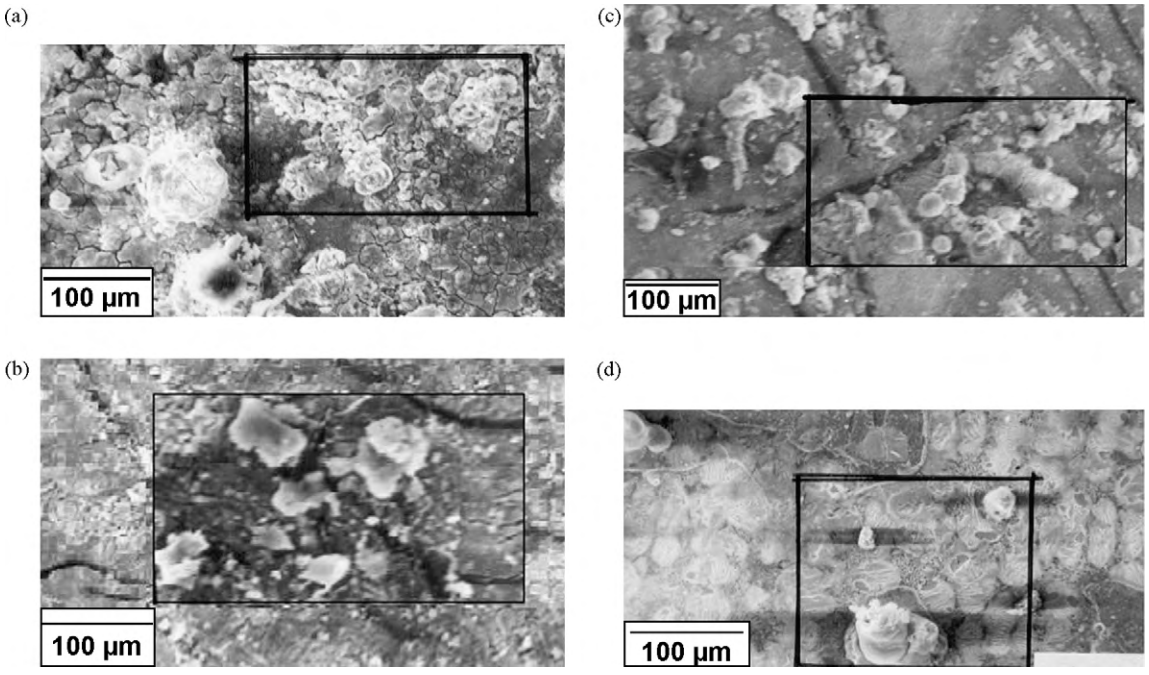

Fig. 12. SEM photomicrograph wear debris of various steels in the mild wear regime. (a) Un-chilled steel. (b) Graphite chilled steel. (c) Copper chilled steel. (d) Subzero chilled steel.

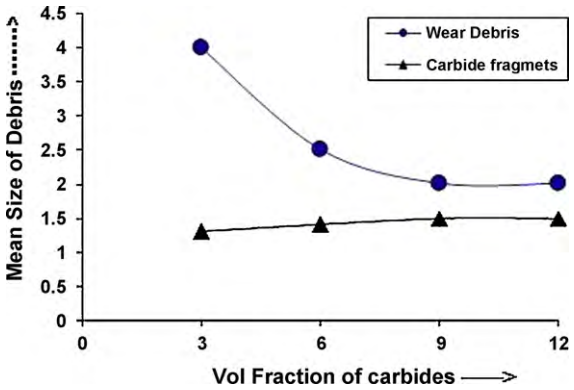

Fig. 13. Plot showing the sizes of wear debris (in μm) and carbide fragments.

3.3.7. Worn surfaces and wear debris

Wear debris generated during the mild wear regime was collected after the end of the wear test and examined under the microscope. SEM photographs of typical wear debris (marked inside the block) are shown in Fig. 12a–d. The shape of the wear debris is mostly large and irregular in the case of the un-chilled steel and in case of chilled steels it was few and fine. From the observations of the worn surfaces and subsurfaces of chilled steels, it is clear that the generation and removal of wear debris is affected by the fragmentation of carbide particles. From SEM studies, it is recognized that carbide particles in wear debris were small and irregular in shape with sharp edges. The mean size of wear debris and the carbide fragments as a function of volume fraction is shown in Fig. 13. It is observed from the results that the size of the wear debris decreases where as the carbide fragments remain more or less the same with increase in volume fraction of carbides. The reason for decrease in the size of the debris is as follows. Under compression, a brittle body is made smaller by crack propagation until a critical size and also due to nonattachment of it to the pearlitic matrix of the material. But the particles below this size are deforming slightly rather than rapid cracking.

Under the mild wear conditions, in particular at the lowest load (10 N), the worn surfaces of the tested chilled steels were characterized by the presence of an oxide compact layer (about 20 μm) comprised of iron oxide. The presence of iron oxide is due to the abrasive action of the pin on the steel counter face. Wear debris collected under conditions were in the form of very fine and rounded particles. XRD and EDS analysis indicated (not shown) that they were mainly comprised of Fe_2O_3. On the contrary, the microstructural observation reveals rough worn surfaces with grooves along the sliding direction were observed in the severe wear regime. They were metallic in appearance, with some dark zones comprised of a mechanical mixed layer [20] containing metallic iron, iron oxides and carbide fragments as confirmed by EDS and XRD analyses. According to Zhang and Alpas [21] in the mild wear regime, always observed at the lowest applied load (10 N), the worn surfaces of both the un-chilled steel and the chilled steels were characterized by the presence of a protective iron oxide rich transfer layer, suggesting that a material transfer process is active. Wear proceeded by spalling of this layer, producing fine and rounded oxide debris. The presence of carbide particles in chilled steels act as a load bearing phase, limiting plastic flow and wear of the matrix. But at the same time plough into the steel abrasive wheel produces debris. These are continuously oxidized during sliding and transferred onto the counter facing sliding surfaces.

Longitudinal cross-sections of the wear scars also analyzed by OM and SEM to characterize the subsurface deformation and to explain the superior wear resistance of the chilled steel with respect to the un-chilled steel. Microhardness tests on the longitudinal cross-sections of the same samples as a function of depth beneath the worn surfaces were carried out in order to evaluate the depth of the affected zone. In the subzero chilled steel with maximum carbide content, two layers were found under the very hard and brittle layer (hardness about 380 HV): a first soft layer (about 150 μm) whose hardness is about 210 HV and a second hardened layer (about 50 μm) with a hardness about 310 HV. These results are in agreement with those obtained by Venkataraman et al. [19], who also observed a soft layer wherein the flow stress decreases with increasing shear strain, followed by a hardening layer, wherein the flow stress increases with increasing strain. The authors related the presence of the soft layer to the formation of ferrite at the coarse pearlite matrix and such ferrite prevent efficient transfer of load from the pearlitic matrix and thus lower the strength of the chilled steels. Conversely, a slight strain-hardening in the shear zone (depth about 250 μm) just beneath the soft layer was found, that the plastic deformation occurred at a higher depth, while the presence of the soft layer was not found.

4. Conclusions

In this research, characterization of wear behavior of different chilled WCB steels including deep cryo-chilled steels cast using high rate heat transfer technique during solidification was studied. The results can be summarized as follows:

1. Microstructure of the chilled steels is finer than that of the un-chilled steel with random orientation of carbide particles in pearlite matrix.
2. Strength, hardness and wear resistance of the chilled steels are superior to those of the un-chilled steel. It was found that these properties increase with an increase in carbide particles in fine pearlite matrix.
3. At lower load, chilled steels exhibited mild wear regime with high coefficient of friction and at higher loads they exhibited severe wear with better wear resistance than the un-chilled steel.
4. Size of the wear debris decreases because of rapid crack propagation of a brittle body under compression where as the size of the carbide fragmentation remain approximately the same.
5. Rate of chilling is identified as an important parameter that affects microstructure and mechanical behavior of WCB steel.

References

[1] J. Hemanth, Mater. Des. 24 (2003) 37–45.
[2] J.Y. Huang, X.Z. Liao, et al., Mater. Sci. Eng. A A339 (2003) 241–244.
[3] D.N. Collins, J. Dormer, Heat Treat. Mater. 23 (1997) 71–76.
[4] R.F. Barron, Prog. Refrig. Sci. Technol. (1973).
[5] F. Meng, K. Tagashira, Scripta Metall. Mater. 7 (1994) 865–868.
[6] A. Bensely, A. Prabhakaran, D. Mohan Lal, G. Nagarajan, Cryogenics 45 (2006) 747–754.
[7] M. Raza Batne, J.A. Szpuran, X. Wang, D.Y. Li, Wear 260 (2006) 116–122.
[8] C. Zhenhua, T. Jie, C. Gang, Y. Hongge, Wear 262 (2007) 362–368.
[9] S. Ahmed, A.S.M.A. Haseeb, A.S.W. Kurny, J. Mater. Process. Technol. 182 (2007) 327–332.
[10] J. Hemanth, Wear 192 (1996) 134–143.
[11] J. Hemanth, Mater. Sci. 33 (1998) 23–35.
[12] Y. Iwai, H. Honda, Wear 181 (1995) 594–602.
[13] D.P. Mondal, S. Das, A.K. Jha, Wear 223 (1998) 131–139.
[14] A.G. Wang, I.M. Hutchings, Mater. Sci. Technol. 5 (1989) 71–84.
[15] S.F. Moustafa, Wear 95 (1995) 185–198.
[16] A. Wang, H.J. Rack, Wear 146 (1991) 337–344.
[17] M.A. Moore, R.M. Douthwaite, Metall. Trans. 7A (1976) 1833–1842.
[18] B.K. Prasad, O.P. Modi, A.K. Jha, Tribol. Int. 27 (1994) 153–158.
[19] B. Venkataraman, G. Sundarajan, Acta Mater. 44 (1996) 451–462.
[20] B.K. Prasad, S. Das, A.K. Jha, Compos. Part A 28A (1997) 301–309.
[21] J. Zhang, A.T. Alpas, Mater. Sci. Eng. 161 (1993) 273–280.